Tenth International Conference on Computational Fluid Dynamics (ICCFD10), Barcelona,Spain, July 9-13, 2018

ICCFD10-047

ALE Seamless Immersed Boundary Method with Overset Grid System for Multiple Moving Objects

Kyohei TAJIRI*, Hidetoshi NISHIDA* and Mitsuru TANAKA*
Corresponding author: tajiri@kit.ac.jp

* Department of Mechanophysics, Kyoto Institute of Technology, Japan.

Abstract: In the Cartesian grid approach, in order to handle the boundary of an object with the complicated shape, the immersed boundary method (IBM) is well used. And, the seamless IBM (SIBM) which improved IBM is also used. In this study, in order to apply the SIBM to multiple moving objects, the SIBM combining the ALE method on the overset grid is proposed. In the overset grid system, a main-grid is generated throughout the computational domain and sub-grids are generated only around each object. Generally, the boundary fitted grid is used for the sub-grid. In this study, the Cartesian grid is used for the sub-grid from the viewpoint of computational efficiency and the SIBM is applied to satisfy the boundary condition. In the present method, in order to handle multiple moving objects, we apply the ALE SIBM only to the sub-grids and move them independently on the main-grid along with each object. In this study, the effectiveness of the present method is discussed. the results by the present method are in good agreement with the results on the single grid. Also, by applying the present method, the grid could be efficiently arranged, and as a result, the number of grid points could be decreased significantly. Therefore, it is concluded that more efficient numerical simulation can be performed for the flow with multiple moving objects by using the present method.

Keywords: Numerical Algorithms, Computational Fluid Dynamics, Turbulence Modeling, Aeroacoustics.

1 Introduction

In recent years, the flow phenomenon handled by the computational fluid dynamics become complicated, and the moving boundary problem is handled more and more. Conventionally, the boundary fitted coordinates are usually adopted for the flow around the object and the grid is regenerated with movement of the object in the moving boundary problem. However, regeneration of the grid increases computational time. Therefore, the Cartesian grid approach is proposed in order to avoid the regeneration of the grid. In the Cartesian grid approach, the immersed boundary method (IBM) [1] is often used due to simplicity of the algorithm. In the IBM, the boundary of an object is represented as a cluster of virtual spots (virtual boundary) and the additional forcing term is added to the momentum equation in order to satisfy the velocity condition on the virtual boundary, e.g., the non-slip condition, and the IBM requires only the position of the virtual boundary on the grid. As for the estimation of the additional forcing term, there are mainly two ways, that is, the feedback [2, 3] and direct [4] forcing term estimations. Generally, the direct forcing term estimation is adopted. However, the conventional IBM with the direct forcing term estimation generates the unphysical pressure oscillations near the virtual boundary because of the pressure jump between inside and outside of the virtual boundary. In order to remove the unphysical pressure oscillations, the seamless IBM (SIBM) [5] was proposed. In the moving boundary problem, whether the IBM or the SIBM is used, it is necessary to update the position of the virtual boundary on the grid with the object moves at each time. Therefore, it increases the computational time. Also, in the case where the object moves in a wide range, it is necessary to generate a fine grid in almost all of the computational domain, and the computational time is greatly increased. In order to solve these problems, the computation of the moving boundary problem was performed more efficiently by combining the arbitrary Lagrangian-Eulerian (ALE) method with the SIBM [6]. In the ALE SIBM, the additional efforts like regeneration of the grid or update the position of the virtual boundary due to movement of the object are not needed because the grid follows the object. Also, no matter how the object moves, it is possible to limit the fine grid to only the vicinity of the object. Then, the moving object can be handled with the same number of grid points as when handling the stationary object. However, because the whole computational grid moves with the object, it has been applied only to a single moving object. Therefore, in this study, we apply the ALE SIBM on the overset grid [7] and try to apply to multiple moving objects. In the overset grid system, since a main-grid is generated throughout the computational domain and sub-grids are generated only around each object, the grids can be aranged efficiently. Generally, the boundary fitted grid is used for the sub-grid. However, in this study, the Cartesian grid is used for the sub-grid from the viewpoint of computational efficiency and the SIBM is applied to satisfy the boundary condition. In the present method, in order to handle multiple moving objects, we apply the ALE method only to the sub-grids and move them independently on the main-grid along with each object. In this study, the effectiveness of the present method is discussed.

2 ALE SIBM with overset grid system

2.1 Governing equations

The governing equations are the continuity equation and the incompressible Navier-Stokes equations based on ALE formulation. In the Navier-Stokes equation based on ALE formulation, the moving velocity of the computational grid is considered in the advective term. And, the forcing term is added to the Navier-Stokes equation for the SIBM. The non-dimensional continuity equation and incompressible Navier-Stokes equations are written as,

$$\frac{\partial u_i}{\partial x_i} = 0, \tag{1}$$

$$\frac{\partial u_i}{\partial t} = F_i - \frac{\partial p}{\partial x_i} + G_i, \tag{2}$$

where, Re denotes the Reynolds number defined by $Re = L_0 U_0/\nu_0$. U_0, L_0 and ν_0 are the reference velocity, the reference length and the kinematic viscosity, respectively. $u_i = (u, v)$ and p are the velocity components and the pressure. G_i in the momentum equations denotes the additional forcing term for the SIBM. F_i denotes the convective and diffusion terms.

$$F_i = -(u_j - c_j)\frac{\partial u_i}{\partial x_j} + \frac{1}{Re}\frac{\partial^2 u_i}{\partial x_j \partial x_j}. \tag{3}$$

Where, c_j is the moving velocity component of the computational grid for ALE method. In this study, $c_j = 0$ at the main-grid because the ALE method is not applied to the main-grid.

2.2 Numerical method

The incompressible Navier-Stokes equation (2) is solved by the second order finite difference method on the collocated grid arrangement. The convective, diffusion and pressure terms are discretized by the conventional second order centered finite difference method. For the time integration, the fractional step approach [8] based on the forward Euler method is applied. For the incompressible Navier-Stokes equations in the IBM, the fractional step approach can be written by

$$u_i^* = u_i^n + \Delta t F_i^n, \tag{4}$$

$$u_i^{n+1} = u_i^* + \Delta t \left(-\frac{\partial p^n}{\partial x_i} + G_i^n \right), \tag{5}$$

where u_i^* denotes the fractional step velocity and Δt is the time increment. The resulting pressure equation is solved by the SOR method.

2.3 Seamless immersed boundary method

In order to adopt the SIBM, the additional forcing term in the momentum equations, G_i, should be estimated. In this paper, the direct forcing term estimation is adopted in accordance with the previous studies [5]. The direct forcing term estimation is shown in Fig. 1. In the figure, I, J are the grid index. We explain in two-dimensions but the extension to three-dimensions is straightforward. For the forward Euler time integration, the forcing term can be determined by

$$G_i^n = -F_i^n + \frac{\partial p^n}{\partial x_i} + \frac{\bar{U}_i^{n+1} - u_i^n}{\Delta t}, \tag{6}$$

where $\bar{U}_i^{n+1}$ denotes the velocity linearly interpolated from the velocity on the near grid point and the velocity (u_{vb}) determined by the velocity condition on the virtual boundary. Namely, the forcing term is specified as the velocity components at next time step satisfy the relation, $u_i^{n+1} = \bar{U}_i^{n+1}$. In the IBM, the grid points added forcing term are restricted near the virtual boundary only (show Fig.1(a)). In this approach, the non-negligible velocity appears inside the virtual boundary. Also, the pressure distributions near the virtual boundary show the unphysical oscillations because of the pressure jump. In the SIBM, the forcing term is added not only on the grid points near the virtual boundary but also in the region inside the virtual boundary shown in Fig1(b) in order to remove the unphysical oscillations near the virtual boundary. In the region inside the virtual boundary, the forcing term is determined by satisfying the relation, $\bar{U}_i^{n+1} = \bar{U}_b$, where $\bar{U}_b$ is the velocity which satisfies the velocity condition at the grid point.

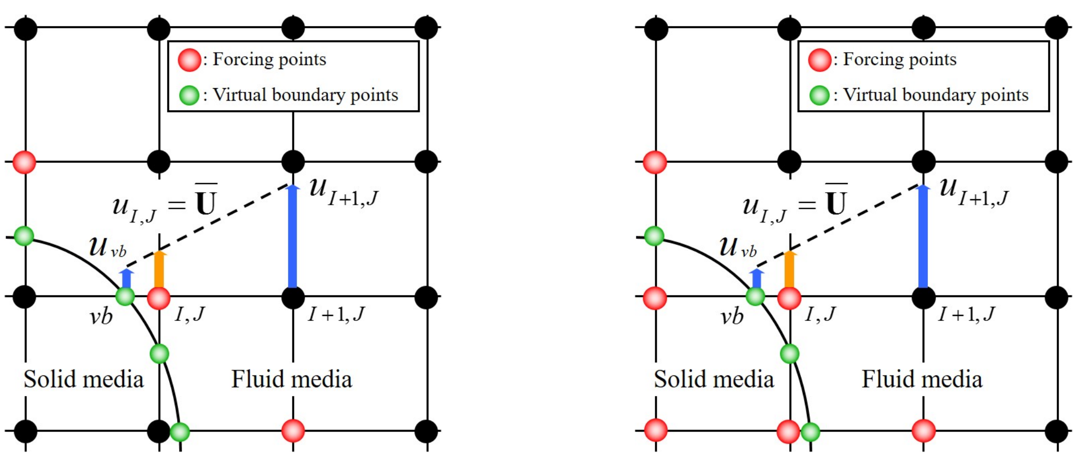

(a) Conventional IBM. (b) Seamless IBM.

Figure 1: Grid points added forcing terms.

2.4 ALE method with overset grid system

In the present method, the overset grid as shown in Fig.2 is used in order to apply ALE SIBM to flow including multiple objects. In order to solve the governing equations on the overset grid, a coarse grid (main-grid) is formed in the whole computational domain, and fine grid (sub-grid) is formed only around an object. And, both the main-grid and the sub-grid are the Cartesian grid. In the present method, there are as many sub-grids as the number of objects. In this study, the ALE SIBM is applied only on the sub-grid. In the present method, on the main-grid, the quantity values in the region overlapping the sub-grid are interpolated from the sub-grid. In addition, the quantity values at the boundary cell on the sub-grid are

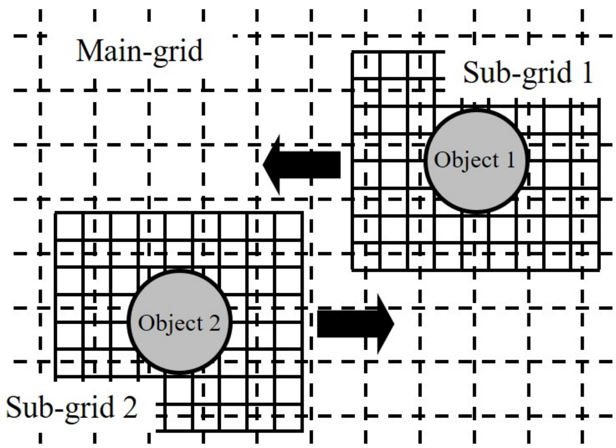

Figure 2: ALE method with overset grid system.

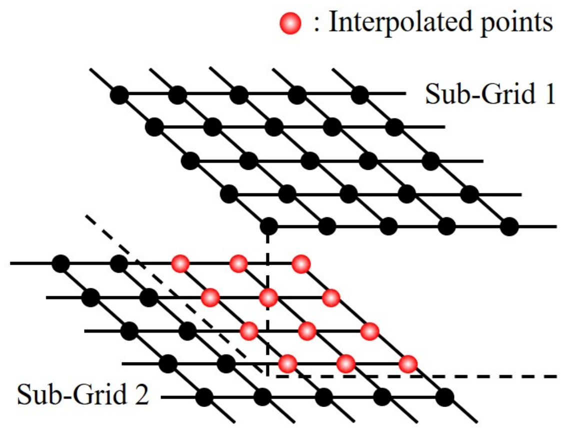

Figure 3: Interpolated points on sub-grid.

similarly interpolated from the main-grid. And, in the present method, it is not interpolated from the sub-grid to other sub-grid. When multiple objects move independently, the sub-grids may overlap each other. In this case, the quantity values at grid points within the region where the sub-grid overlaps each other are interpolated from the main-grid as shown in Fig.3.

3 Application to two moving 2D circular cylinders

In order to validate the present method, two moving two-dimensional circular cylinders in the domain surrounded by the wall are considered (see Fig.4). These cylinders translate on the circumference with the diameter $D = 1.8$ and the tangential velocity is 1, ie the period of motion is 1.8π. The coordinates of the center of each circular cylinder are represented by

$$\theta = \frac{2t}{D}, \tag{7}$$

$$x_1 = \frac{D}{2}cos\theta + 2.5, \qquad y_1 = \frac{D}{2}sin\theta + 2.5, \tag{8}$$

$$x_2 = \frac{D}{2}cos(\theta + \pi) + 2.5, \qquad y_2 = \frac{D}{2}sin(\theta + \pi) + 2.5. \tag{9}$$

As for the computational grid, the computational result by the present method (on the overset grid) is compared with the result on the single grid. In the single grid, the calculation is performed in the case where the grid resolution is 0.025 (single-1) and 0.0125 (single-2). In the overset grid, the grid resolution of the main-grid is 0.025, and the calculation is performed in the case where the grid resolution of the sub-grid is 0.025 (overset-1), and 0.0125 (overset-2), The sub-grid is a square whose side is 1.6 and the circular cylinder is positioned at the center of the square. The number of grid points is 40000 (200×200) for the single-1 and 160000 (400×400) for the single-2. In the present method, the number of grid points is 48192 (main-grid : 200×200, sub-grid : 64×64) for the overset-1 and 72768 (main-grid : 200×200, sub-grid : 128×128) for the overset-2. Where note that there are as many sub-grids as the number of cylinders. In the overset-1, because the resolutions of the main-grid and the sub-grid are the same, the number of grid points increases more than in the single-1. In the overset-2, because the resolution of the main-grid is coarser than the resolution of the sub-grid, the number of grid points decreases significantly more than in the single-2. When the sub-grids follows the circular cylinder under these conditions, the sub-grids may overlap each other as shown in Fig.5. On the wall boundary, the velocity is imposed by the non-slip condition and the pressure is imposed by the Neumann condition obtained by the normal momentum equation. The Reynolds number is set as $Re = 100$.

Figure6-8 show the streamlines and the vorticity contours and the pressure contours at overset-2. Figure9 shows the pressure contours and the grid arrangement near the cylinder. From Fig.6, it can be seen that the

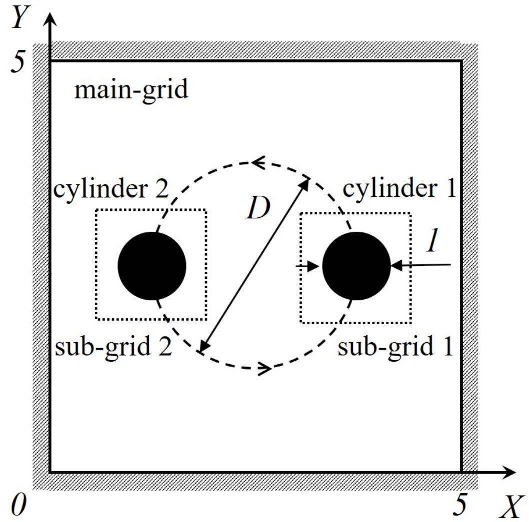

Figure 4: Computational domain.

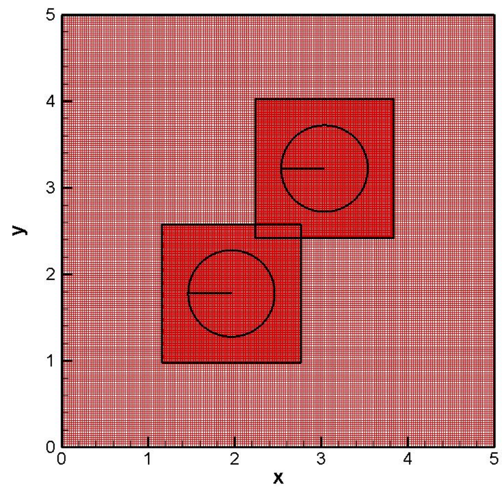

Figure 5: Grid layout.

flow is generated by the movement of the cylinders. From Figs7, 8, it can be seen that the point-symmetric distributions are obtained. Therefore, it is considered that a reasonable analysis result was obtained. In Fig.9, it can be seen that the pressure distributions are smoothly connected between the grids. Therefore, it is considered that present method could be appropriately applied.

Figure10 shows the comparison of the time history of the X-component of the fluid force coefficients of each grid system. Where the horizontal axis represents the cycle of movement of the cylinders. The X-component of the fluid force coefficients can be determined by

$$CF_x = \frac{-\int_O \left(G_x - u_i \frac{\partial u}{\partial x_i} - \frac{\partial u}{\partial t} \right) ds}{\frac{1}{2}\rho_0 U_0^2 d}, \tag{10}$$

where O denotes the region to which the forcing term is added in the SIBM and d denotes the diameter of each cylinder. Periodic results corresponding to the movement of each cylinder are obtained. The phase of results at each cylinder is shifted by a half cycle because each cylinder is positioned point-symmetrically. The obtained coefficients are in good agreement between the single-1 and the overset-1 or the single-2 and the overset-2 which have the same grid resolution near the cylinder. Therefore, it was shown that effective results can be obtained even when the fine grid is limited to only near the cylinder by the present method. Also, in the single-1, the occurrence of oscillations in the time history of the fluid force coefficients is remarkable. This is because the position of the virtual boundary has been updated on the coarse grid. In the overset-1 with the same grid resolution as the single-1, the oscillations are suppressed to the same extent as the single-2 and the overset-2. This is because the overset-1 by the present method does not require updating the position of the virtual boundary. Therefore, it was shown that oscillations in time history of fluid force coefficients can be suppressed even with relatively coarse grid resolution by applying the present method.

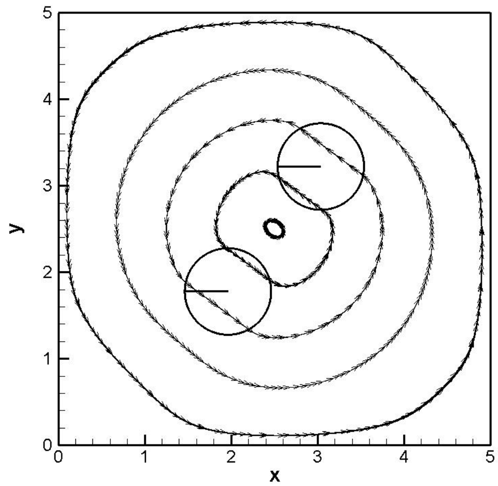

Figure 6: Streamlines at overset-2.

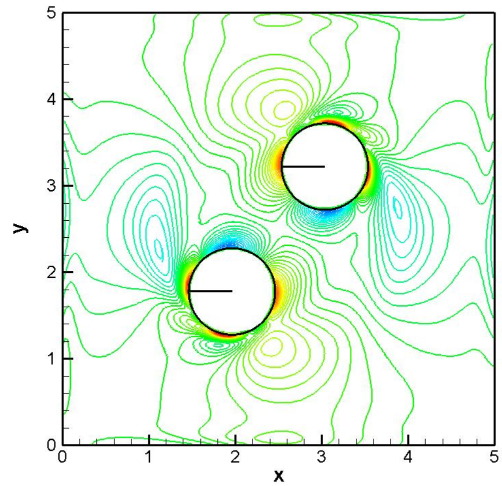

Figure 7: Vorticity contours at overset-2.

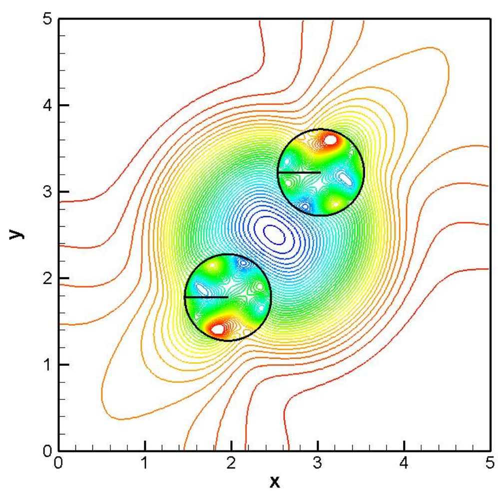

Figure 8: Pressure contours at overset-2.

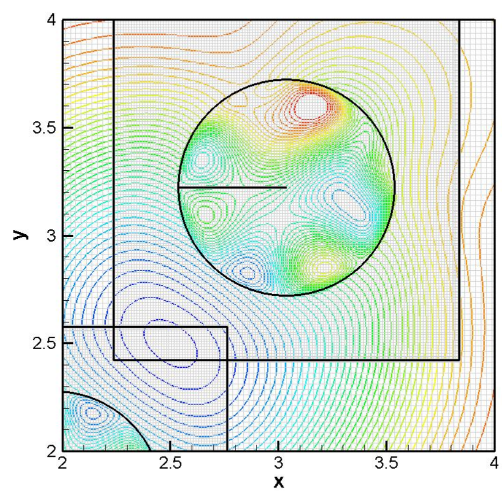

Figure 9: Closeup view of pressure contours and grid layout at overset-2.

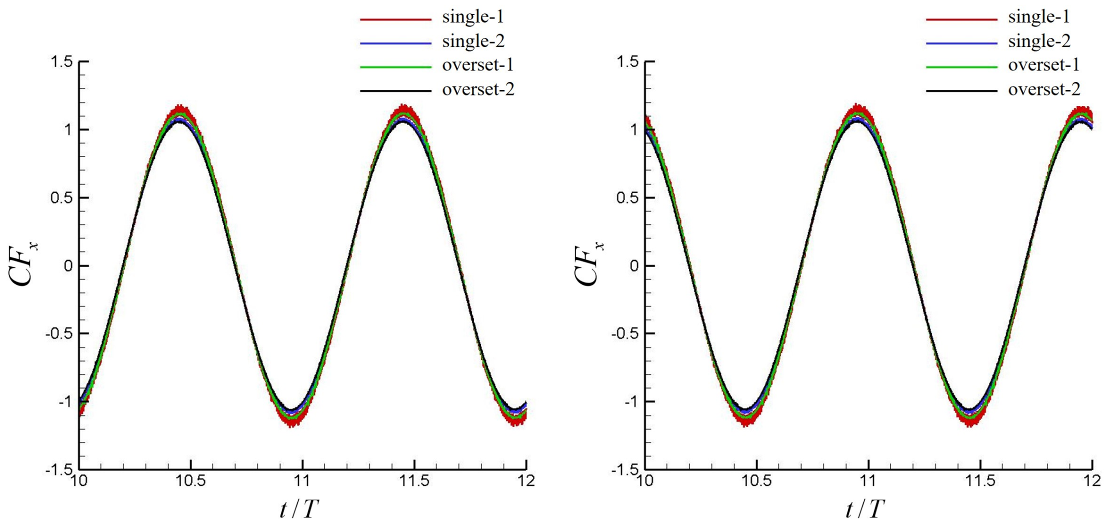

(a) cylinder 1 (b) cylinder 2

Figure 10: Time history of the X-component of the fluid force coefficient.

4 Application to two moving spheres

In this chapter, the present method is extended to three-dimensions and the two moving sphere in the domain surrounded by the wall as shown in the Fig.11 are considered. These spheres translate on the circumference with the diameter $D = 2$ on the $x = y$ plane and the tangential velocity is 1, ie the period of motion is 2π. The coordinates of the center of each sphere are represented by

$$\theta = \frac{2t}{D}, \tag{11}$$

$$x_1 = y_1 = \frac{D}{2\sqrt{2}}cos\theta + 2.0, \qquad z_1 = \frac{D}{2}sin\theta + 2.0, \tag{12}$$

$$x_2 = y_2 = \frac{D}{2\sqrt{2}}cos(\theta + \pi) + 2.0, \qquad z_2 = \frac{D}{2}sin(\theta + \pi) + 2.0. \tag{13}$$

As for the computational grid, the grid resolution is 0.025 (single-1) in the single grid. In the overset grid, the grid resolution of the main-grid is 0.025, and the calculation is performed in the case where the grid resolution of the sub-grid is 0.025 (overset-1), and 0.0125 (overset-2), The sub-grid is a cube whose side is 1.6 and the circular cylinder is positioned at the center of the cube. The number of grid points is 4096000 ($160 \times 160 \times 160$) for the single-1. In the present method, the number of grid points is 4620288 (main-grid : $160 \times 160 \times 160$, sub-grid : $64 \times 64 \times 64$) for the overset-1 and 8290304 (main-grid : $160 \times 160 \times 160$, sub-grid : $128 \times 128 \times 128$) for the overset-2. In this calculation, the single grid with grid resolution of 0.0125 (single-2) is not handled, but the number of grid points is 32768000. In overset-2 applying the present method under the above conditions, the number of grid points is about a quarter of single-2. On the wall boundary, the velocity is imposed by the non-slip condition and the pressure is imposed by the Neumann condition obtained by the normal momentum equation. The Reynolds number is set as $Re = 100$.

Figure12 show the vortex structures by using iso-surfaces of the second invariant of velocity gradient tensor ($Q^{'} = 0.1$). The black lines in the figure represent grid boundaries. At this time, the sub-grids partially overlap each other. The point-symmetric distributions can be confirmed, and the smoothly connected distributions are obtained among each grid. Figure13 shows the comparison of the time history of the X-component of the fluid force coefficients of each grid system and Fig.14 shows the closeup view thereof. Periodic results corresponding to the movement of each sphere are obtained and the phase of results at each cylinder is shifted by a half cycle because each sphere is positioned point-symmetrically. The obtained coefficients are in good agreement between the single-1 and the overset-1 which have the same grid resolution near the sphere. Furthermore, in the overset-1 and the overset-2 applying the present method, the oscillations are suppressed more than the single-1. Therefore, also in the three-dimensional analysis, the effect of suppressing the oscillations in the time history of the quantitative value by the present method was confirmed.

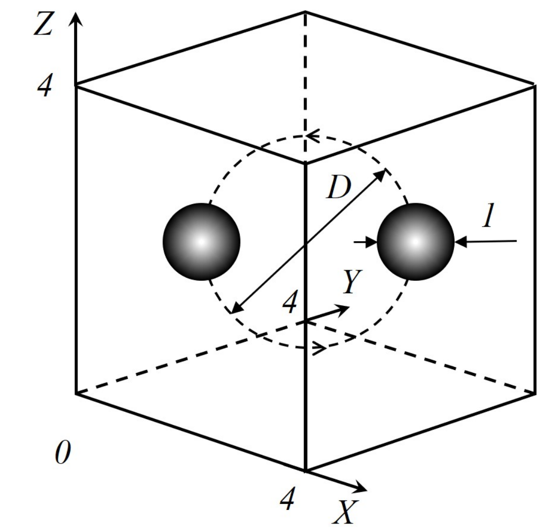

Figure 11: Computational domain.

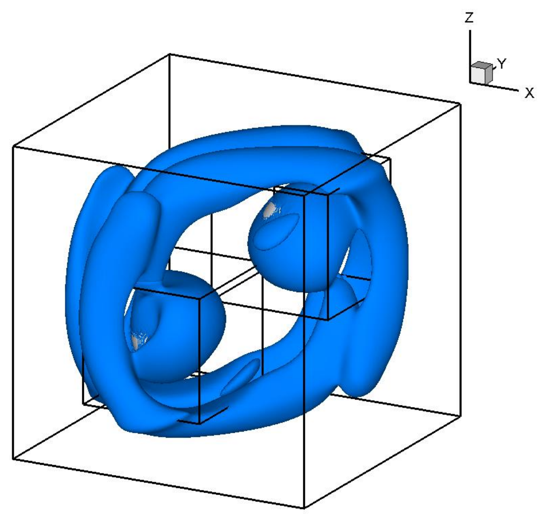

Figure 12: Iso-surface of second invariant of velocity gradient tensor ($Q^{'} = 0.1$).

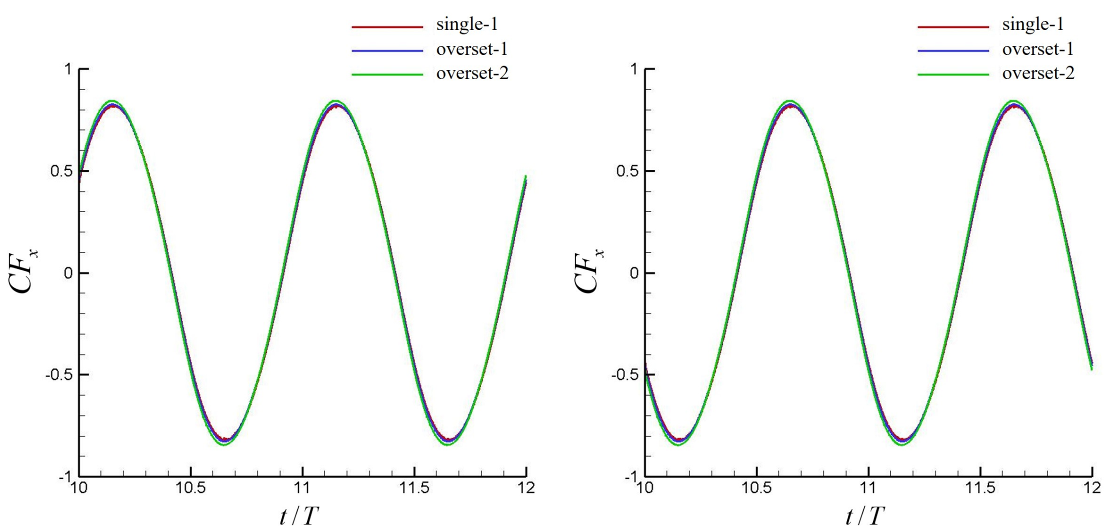

(a) sphere 1

(b) sphere 2

Figure 13: Time history of the X-component of the fluid force coefficient.

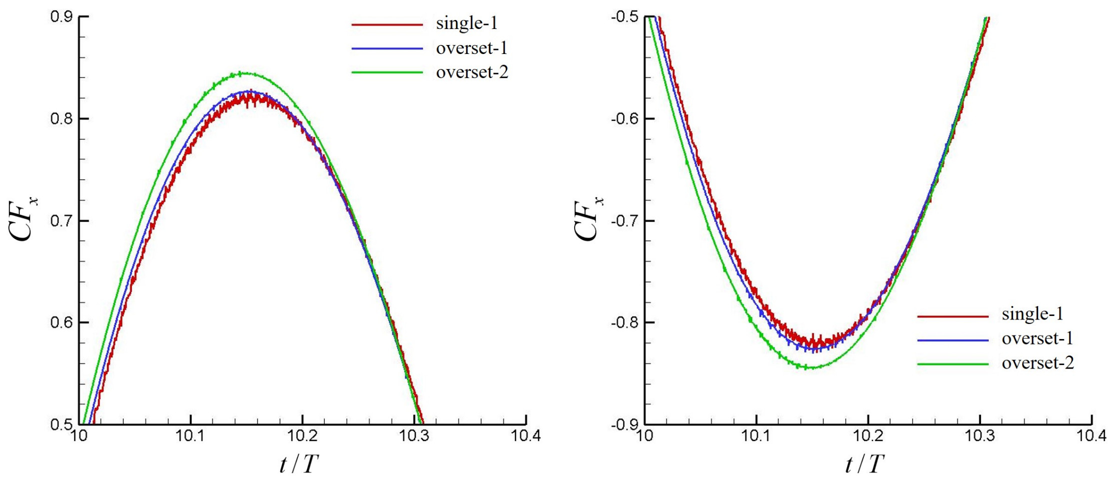

(a) sphere 1

(b) sphere 2

Figure 14: Closeup view of time history of the X-component of the fluid force coefficient.

5 Concluding Remarks

In this study, we proposed the ALE SIBM with overset grid system for multiple moving objects. In the present method, in order to handle multiple moving objects, we apply the ALE method only to the sub-grids and move them independently on the main-grid along with each object. As a result, even when multiple objects move independently, the fine grid can be generated only near the virtual boundary. In order to verify the present method, two two-dimensional cylinders and spheres were considered, respectively. By applying the present method, the grid could be efficiently arranged, and as a result, the number of grid points could be decreased significantly. Also, the results by the present method are in good agreement with the results on the single grid. Therefore, it is concluded that more efficient numerical simulation can be performed for the flow with multiple moving objects by using the present method. Furthermore, it was shown that oscillations in time history of fluid force coefficients can be suppressed even with relatively coarse grid resolution by applying the present method. Then, it is concluded that the ALE SIBM with overset grid system is very promising for multiple moving objects.

References

[1] C. S. Peskin and D. M. McQueen. A three-dimensional computational method for blood flow in the heart I. immersed elastic fibers in a viscous incompressible fluid. *Journal of Computational Physics*, 81(2):372–405, 1989.

[2] D. Goldstein, R. Handler, and L. Sirovich. Modeling a No-Slip Flow Boundary with an External Force Field. *Journal of Computational Physics*, 105(2):354–366, 1993.

[3] E. M. Saiki and S. Biringen. Numerical Simulation of a Cylinder in Uniform Flow : Application of a Virtual Boundary Method. *Journal of Computational Physics*, 123(2):450–465, 1996.

[4] E. A. Fadlun, R. Verzicco, P. Orlandi, and J. Mohd-Yosof. Combined immersed-boundary finite-difference methods for three-dimensional complex simulations. *Journal of Computational Physics*, 161(1):35–60, 2000.

[5] H. Nishida and K. Sasao. Incompressible Flow Simulations Using Virtual Boundary Method with New Direct Forcing Terms Estimation. *Proceedings of International Conference on Computational Fluid Dynamics 2006*, pages 185–186, 2006.

[6] K. Tajiri, H. Nishida, and M. Tanaka. Large Eddy Simulation of Turbulent Flow using Seamless Immersed

Boundary Method. *Proceedings of 8th International Conference on Computational Fluid Dynamics*, (0197):1–13, 2014.

[7] J.A. Benek, P.G. Buning, and J.L. Steger. A 3-D chimera grid embedding technique. *AIAA Paper*, (85-1523), 1985.

[8] C.M. Rhie and W.L. Chow. Numerical Study of the Turbulent Flow Past an Airfoil with Trailing Edge Separation. *AIAA Journal*, 21(11):1525–1532, 1983.